**Charles University**

**Faculty of Science**

Study programme: Biochemistry


**Martin Sojčiak**

# Enzyme kinetics of the HelD protein

Enzymová kinetika proteinu HelD

Bachelor's thesis

Supervisor: **Ing. Jan Dohnálek, Ph.D.**

Consultant: **RNDr. Petr Pompach, Ph.D.**

Prague, 2025

**Declaration**

I declare that I have prepared the thesis independently and that I have listed all the information sources and literature. Neither this thesis nor any substantial part of it has been submitted for another or the same academic degree. During the preparation of this bachelor's thesis, I used Grammarly and ChatGPT to correct grammar, improve the clarity of the text, and search for relevant literature. After using these tools, I have reviewed and edited the content as necessary and take full responsibility for the final content of the publication.

Prague, 16. 5. 2025 Martin Sojčiak

**Acknowledgment**

I would like to thank my supervisor, Ing. Jan Dohnálek, Ph.D., for his help, guidance, and valuable insights throughout this thesis. I also want to thank my consultant, RNDr. Petr Pompach, Ph.D., for his valuable input for this work. Thanks as well to everyone in the Laboratory of Structure and Function of Biomolecules of the Institute of Biotechnology. Finally, thanks to the grant projects Czech Science Foundation, no. 23-06295S and 25-16037S, which made this thesis possible.

# Abstract

Mycobacterial HelD is a protein responsible for the dissociation of RNA polymerase from nucleic acids during stalled transcription. Subsequent release of HelD from RNAP can be achieved through ATP and GTP hydrolysis by HelD. Notably, HelD exhibits catalytic activity independent of RNA polymerase. This thesis identifies optimal reaction conditions to maximize the hydrolysis rate and characterizes the enzyme kinetics under these conditions. Furthermore, a modified substrate inhibition equation is proposed to describe the observed substrate inhibition, providing a model for the inhibitory effects at high substrate concentrations.



# Keywords

Transcription factor HelD, bacterial RNA polymerase, enzyme kinetics, substrate inhibition



# Abstrakt

Mykobakteriální HelD je protein zodpovědný za disociaci RNA polymerázy od nukleových kyselin během zastavené transkripce. Následné uvolnění HelD z RNA polymerasy lze dosáhnout hydrolýzou ATP a GTP v HelD. Pozoruhodné je, že HelD vykazuje katalytickou aktivitu i když není asociován s RNA polymerásou. Tato práce stanovuje optimální reakční podmínky pro maximalizaci rychlosti reakce a charakterizuje kinetiku enzymu za těchto podmínek. Dále je navržena modifikovaná rovnice pro inhibici substrátem jako model, popisující pozorované inhibiční účinky vysokých koncentrací substrátu.



# Klíčová slova

Transkripční faktor HelD, bakteriální RNA polymerasa, enzymová kinetika, inhibice substrátem [V angličtině]

# List of Abbreviations

| | |
|---|---|
| AMP-PNP | adenosine 5'-(β,γ-imido)triphosphate |
| Cryo-EM | cryogenic electron microscopy |
| dwDNA | downstream DNA |
| DTT | Dithiothreitol |
| *E. coli* | *Escherichia coli* |
| EDTA | ethylenediaminetetraacetic acid |
| *Msm* | *Mycobacterium smegmatis* |
| ES | enzyme-substrate complex |
| NTP | nucleoside triphosphate |
| (p)ppGpp | guanosine pentaphosphate and tetraphosphate |
| SAXS | small angle X-ray scattering |
| SEC | size exclusion chromatography |
| SDS-PAGE | sodium dodecyl sulfate–polyacrylamide gel electrophoresis |
| TCEP | tris(2-carboxyethyl)phosphine |
| TEV | Tobacco Etch Virus |

# Contents

# 1 Introduction

## 1.1 RNA polymerase

For a bacterium to make its own proteins from its DNA (express its genes), it needs to go through a series of steps. The very first step in this gene expression is the transcription of DNA template into RNA. In prokaryotes, getting the RNA from DNA is the responsibility of the RNA polymerase (RNAP) protein complex. This complex is composed of a catalytic core consisting of at least five subunits ($\alpha_2$, $\beta$, $\beta$', $\omega$) and a $\sigma$ factor[1].

The catalytic core of RNAP is responsible for synthetising RNA and terminating transcription at appropriate sites[2]. During RNA synthesis, ribonucleoside 5'-triphosphates are added to a growing RNA strand in the 5' to 3' direction, guided by the complementary bases from the DNA template[3]. RNAP catalyzes the formation of phosphodiester bonds between ribonucleotides through a nucleophilic attack by the 3'-OH group of the last nucleotide in the RNA chain on the 5'-triphosphate group of the incoming ribonucleotide[4].

This catalytic reaction takes place in the primary channel of RNAP which is formed mostly by $\beta$ and $\beta$' subunit. These two subunits create a shape that resembles a crab's claw (Figure 1). RNAP also contains a secondary channel through which ribonucleoside 5'-triphosphates enter and an exit channel through which nascent RNA leaves the complex[5].

In bacteria, RNA synthesis begins only in specific regions of DNA called promoters. For RNAP to start transcribing DNA, it must first recognize this region, and create a complex with the DNA. This is the role of the $\sigma$ factor which associates with the catalytic core to create the RNAP holoenzyme[6]. In addition to recognizing the promoters and creating the "closed" complex, it also stabilizes the open complex[7]. The open complex is the structure that forms when the RNAP binds to the promoter and the DNA strands have been unwound, allowing transcription to begin[8].

For bacteria to use their resources efficiently and adapt to environmental changes, they need some mechanisms to regulate transcription. This is mostly achieved by the interaction of RNAP with various molecules and factors, such as NTPs[9], small RNA molecules[10], and proteins[11][12]. It can also be regulated indirectly, e.g. alarmones (p)ppGpp affect the

concentration of ATP and GTP which regulate RNAP directly[13].

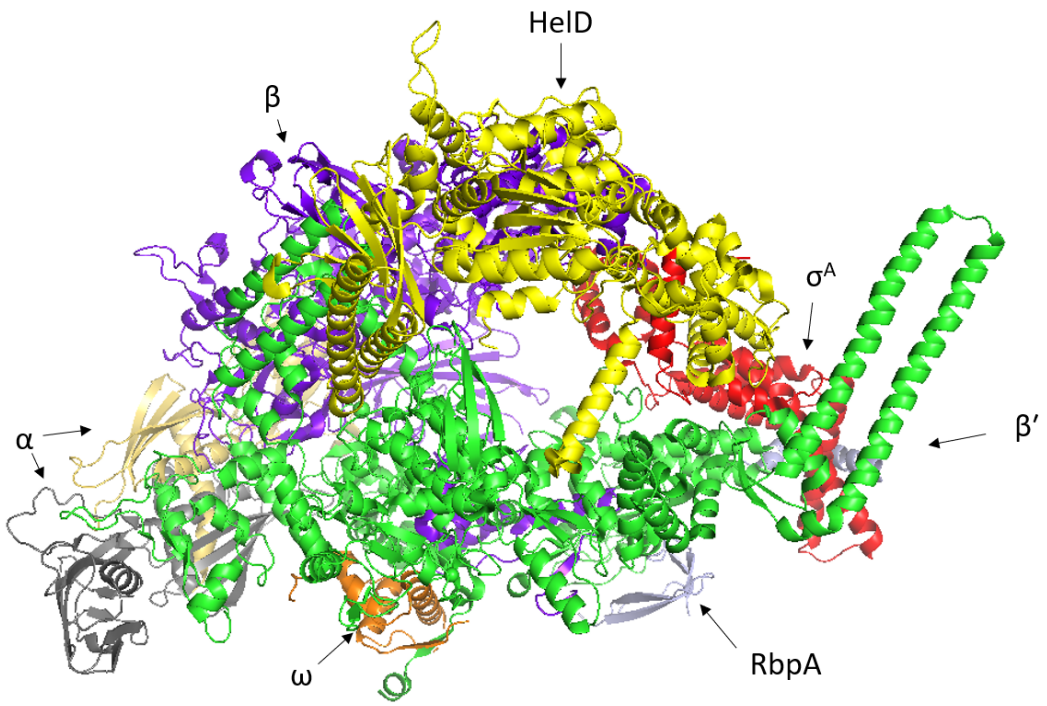


Figure 1: Structure of *Msm* RNAP with $\sigma^A$, RbpA and HelD in state I (PDB: 8Q3I[14]) determined by cryo-EM single particle analysis. The individual subunits and transcription factors of RNAP are differentiated by color and marked

## 1.2 HelD

### 1.2.1 Discovery of HelD

HelD as a transcription factor was first discovered in a study aimed at how RNAP from *Bacillus subtilis* interacts with other proteins during different growth phases and in different stress conditions[15]. Based on sequence homology it belongs to the superfamily 1 (SF1) of DNA and RNA helicases[16]. These helicases unwind DNA in either 3'-5' (SF1A) or 5'-3' (SF1B) direction, relying on energy supplied by ATP[17].

At first, it was assumed that HelD takes a role in DNA repair and homologous recombination because, during UV-induced DNA damage, the lack of HelD in *Bacillus subtilis* had a negative effect[18]. However, there was no concrete biochemical evidence for this and the exact function remained unknown.

An important milestone in explaining the function of HelD was achieved when a study

proved that HelD interacts with RNAP, and found the place of RNAP to which it binds, confirming the role HelD plays in transcription[16]. Furthermore, it found that HelD in co-operation with another RNAP factor δ, helps the transcription by releasing nonfunctional RNAP from DNA, this process was shown to be dependent on ATP[16].

SEC and SAXS analysis showed that *B. subtilis* HelD is predominantly a globular monomer in solution[19]. In addition to its monomeric form, evidence from AUC and SEC in the same study found that HelD tends to form higher-order oligomers.

Further SAXS analyses of HelD were able to give first insights into the domain structure of HelD and observed a conformational change upon binding of the substrate analog AMP-PNP[20]. This study also showed that HelD binds to the primary and secondary channels, forming a previously unprecedented complex that prevents the binding of anything else in the RNAP. Better insights into the structure of HelD were obtained using cryo-EM. The obtained structural data showed how HelD could possibly recycle RNAP, through these conformational changes. The data also showed that in *Msm*, HelD binding to RNAP does not exclude the presence of $\sigma^{A}$ factor[21]. This has been demonstrated by other cryo-EM studies, where the RNAP complex with HelD sigma A and RbpA was successfully crystallized[14]. Here, the authors were able to discover what role HelD plays in transcription initiation and were also able to clarify how HelD decouples from RNAP.

Even before HelD was discovered as a protein, the gene encoding HelD was shown to be inducible by antibiotic rifampicin[22]. It was later confirmed that HelD can indeed confer resistance to the rifampicin[23]. In experiments with sublethal doses of rifampicin, three different phenomena indicative of rifampicin resistance induced by HelD were observed. HelD is expressed 25-fold higher than normal when exposed to rifampicin, HelD associates with RNAP at an increased rate under these conditions, and the deletion of the HelD gene results in increased sensitivity to rifampicin[24 23].

There are three known classes of HelD in bacteria, class I in the low G+C Gram-positives (such as *Bacillus subtilis*), class II in the high G+C Gram-positives (such as *Msm*), and class III in certain Gram-negative bacteria[25]. These classes differ in structural features (such as the primary channel loop) and the mechanism by which they remove nucleic acids and recycle RNAP. This thesis will deal only with *Msm* HelD and therefore

only with class II HelD proteins.

### 1.2.2 Structure and function of *Msm* HelD

HelD consists of five structured domains/regions: N-terminal (N-term) domain, NTPase 1A–2A heterodimer (1A domain is separated into two parts: 1A-1 and 1A-2 in the primary sequence of amino acids), clamp opening domain (CO-domain), and the primary channel loop (PCh loop) feature[21].

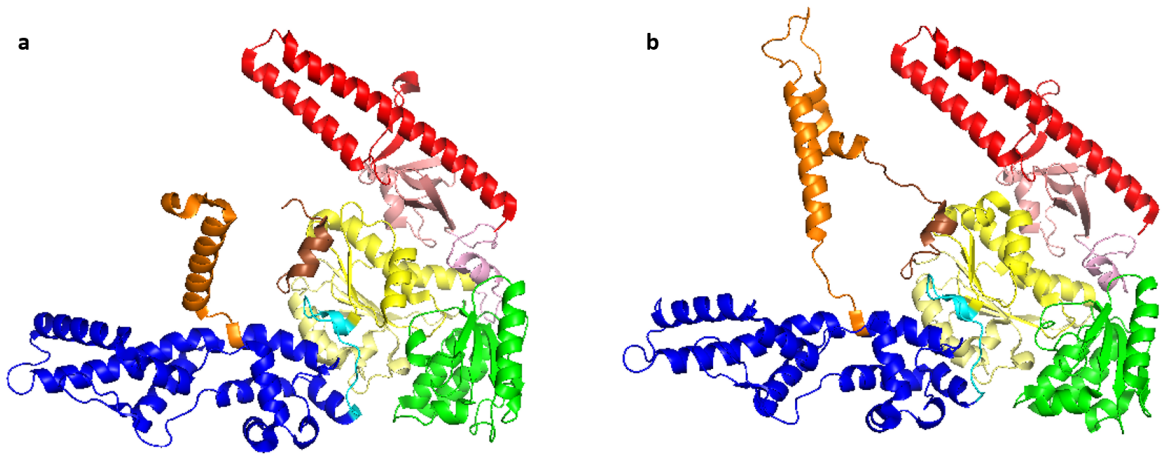


Figure 2: HelD in the state I (**a**), and in state II (**b**) (PDB: 8Q3I[14]) color coded accordingly: PCh loop (orange), CO domain (blue), CO-linker(light blue), 1A domain (green), 2A domain (yellow), N-terminal domain (red), NG domain(pink).

The structure of HelD resembles an arc that fits RNAP (Figure 2). One end of the arc (CO domain) is inserted into the primary channel. This blockage of the primary channel prevents the presence of nucleic acids[21]. It also causes the RNAP clamp to widen by 35 Å, which is even more than some measured forms of RNAP-antibiotic complexes[26,27]. The binding of the CO domain to the primary channel of RNAP results in conformational changes, which change the fold of the CO domain, making the RNAP clamp even wider, and causing the primary channel loop to refold. This refolded primary channel loop interferes with the active site of RNAP, which makes the addition of nucleotides to RNA impossible. HelD binding also widens the RNA exit channel which facilitates the exit of RNA from RNAP.

The other end (the N-terminal domain in the form of antiparallel coiled-coil) inserts into the secondary channel from where NTPs come into the RNAP for RNA synthesis, but

it does not cover the channel well enough to keep the nucleotides from coming. It does, however, induce a conformational change in β' trigger loop, which prevents nucleotide addition to growing RNA[21].

The function of HelD is to recycle stalled RNAP if RNAP does not successfully leave DNA, or if the elongation complex gets stalled. HelD binds to RNAP using its N-terminal domain which causes conformational changes as described above and destabilizes the binding of dwDNA. This dwDNA destabilization enables the CO domain to bind to the primary channel which empties the active site as described above. Biochemical studies show that the disassembly of RNAP elongation complex does not depend on ATP hydrolysis[21].

For the recycled RNAP to continue transcribing DNA into RNA, it needs to remove HelD. HelD needs energy to release from RNAP[14]. This energy is obtained either by hydrolysis of NTP in 1A-2A heterodimer or by the formation of a bond between RNAP and DNA[20]. This heterodimer is a conserved NTPase Rossmann fold domain similar to other proteins of the SF 1 superfamily of helicases, except that it lacks certain motifs for binding DNA. Biochemical data show that HelD releases from RNAP at approximately equal rates for 1 and 8 mM ATP[14]. The protein shows NTPase activity with NTPs with purine bases but lacks NTPase activity toward NTPs with pyrimidine bases.

Current structural data of HelD do not show this active site in a state compatible with binding NTPs. When the active site of HelD is superimposed with the active site of UvrD with bound AMP-PNP (Figure 3), corresponding active site residues are not in conformation that would allow binding NTP. Furthermore, in class II HelD, access to the active site is obstructed by a structural element from an adjacent domain, as shown in Figure 3.

The other function of HelD is protection against rifampicin as mentioned in the previous section. Rifampicin works by binding to the β subunit in the DNA-RNA channel of RNAP. Bound rifampicin prevents the RNA from elongating to more than 3 nucleotides during transcription, on the other hand, if the RNA has more than three nucleotides, then rifampicin binding is prevented[28 29 30].

HelD protects the bacterium from rifampicin not only by releasing the stalled RNAP from the DNA but it is also able to expel the rifampicin itself from the polymerase[24].

This expulsion is dependent on the Pch loop, which is specific to class II HelD, this group also includes *Msm* HelD[30]. When HelD goes from state I (Figure 2a) into state II (Figure 2b), the PCh loop extends to the active site and near the rifampicin binding pocket of RNAP and changes its conformation. This causes amino acid residues to interact in a way that causes deformation of this pocket. This deformation is responsible for the fact that the simultaneous binding of both rifampicin and HelD would cause atomic clashes. HelD is then responsible for the displacement of rifampicin from RNAP, this is achieved by conformational changes to RNAP caused by hydrolysis of ATP in HelD, and also by HelD taking over the hydrogen bonding to RNAP from rifampicin, these two causes destabilize the binding of rifampicin and reduce its affinity for RNAP[30]. There is no change or degradation of the antibiotic, which means this protection is temporary, only as long as HelD is bound to RNAP. Furthermore, HelD can expel rifampicin without causing RNAP to disengage from promoter DNA, allowing RNAP to resume transcription more quickly. This cycle can repeat until transcription proceeds successfully despite the presence of rifampicin[14].

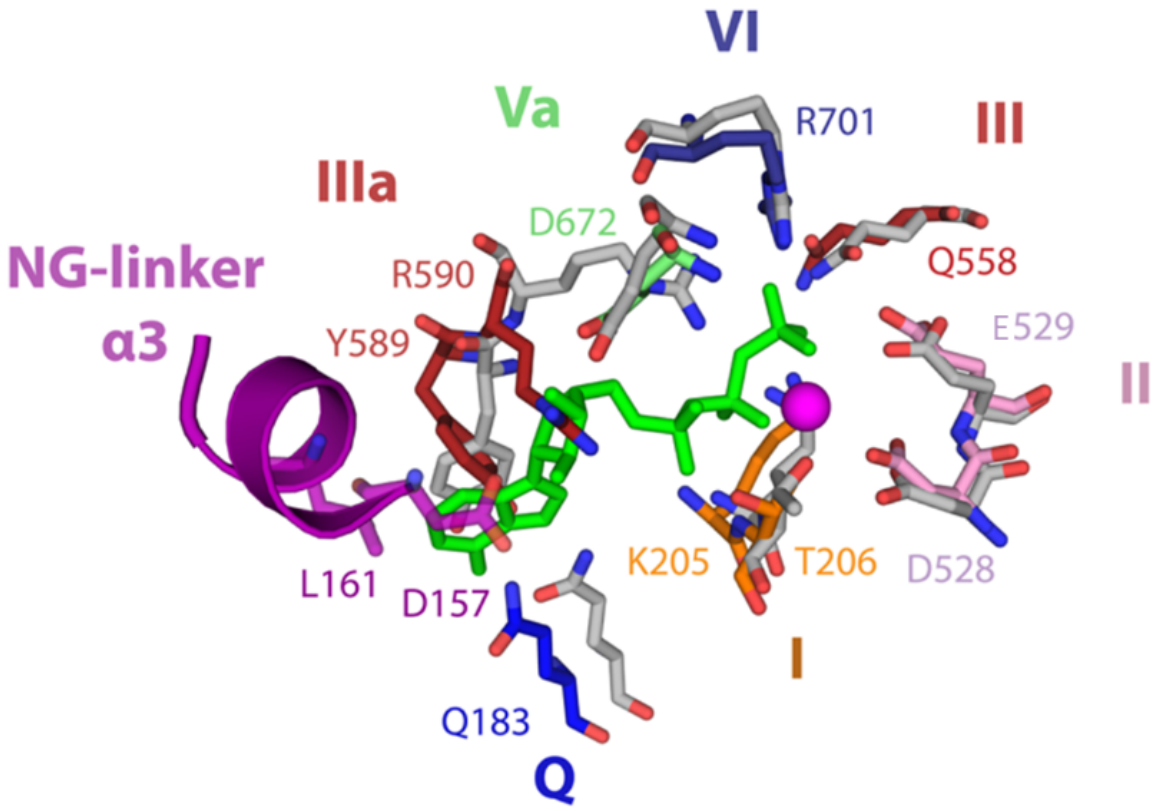


Figure 3: Superposition of the HelD NTP-binding site in state I (color coded, PDB: 8Q3I[14]) and the UvrD ATP-PNP-bound state (grey, PDB: 2IS4[31]). I, II, III, IIIa, Va, VI, and Q are the nucleotide binding motifs. Conserved residues are present but not in conformations compatible with NTP binding. The NG-linker forces Y589 and R590 residues to clash with the base and ribose of NTP and obstruct access to the active site, making the binding and hydrolysis of NTPs impossible in this state of HelD.

## 1.3 Enzyme kinetics

Enzyme kinetics is a discipline that investigates enzymes by determining the rates of reactions and analyzing changes in these rates under differing reaction conditions, to study the properties of the enzymes, such as substrate specificity, affinity, and regulation.

At the core of enzyme kinetics lies the dependence of enzymatic activity on the substrate concentration. This dependence was explained and quantified by L. Michaelis and M. Menten, who claimed that the enzyme first creates an enzyme-substrate complex in a fast reversible reaction and then creates a product in a slower second reaction, leaving the original enzyme unchanged in the end[3]. The kinetic curve describing the dependence between substrate concentration and the rate of a reaction can be expressed by the Michaelis-Menten equation:

$$v = \frac{V_{\max}[S]}{K_{\mathrm{m}} + [S]} \tag{1}$$

Where $V_{\max}$ is the highest possible rate of the reaction when the enzyme is saturated with the substrate and the $K_{\mathrm{m}}$ is the substrate concentration at which the reaction rate reaches half of its maximum velocity. $K_{\mathrm{m}}$ is a helpful kinetic parameter, which tells about the enzyme's affinity for its substrate, the higher the $K_{\mathrm{m}}$ value the lower the affinity.

In addition to the Michaelis-Menten model, in the presence of inhibitors, more complex behavior, such as reversible and irreversible enzyme inhibition can occur. In reversible inhibition, the enzyme associates with the inhibitor through non-covalent interactions. Reversible inhibitors can dissociate from the enzyme, restoring its activity, unlike irreversible inhibitors, which bind to the enzyme covalently. Reversible inhibition is a crucial tool for enzymatic regulation in all organisms. There are three major types of reversible inhibition: competitive, uncompetitive, and mixed inhibition. Each type affects enzymatic parameters differently[3].

The competitive inhibitory model describes inhibitors, which compete with the substrate for the active site. This increases the apparent $K_{\mathrm{m}}$ but does not affect $V_{\max}$. This inhibition can be reversed by adding more substrate.

The uncompetitive inhibitory model describes inhibitors, which bind only to enzyme-substrate complex, preventing the reaction from proceeding to product formation. This reduces both $K_{\mathrm{m}}$ and $V_{\max}$, and the effect cannot be reversed by increasing the substrate concentration.

Mixed inhibition is an inhibition, where the inhibitor binds both to the enzyme and the enzyme-substrate complex. It usually affects both $K_{\mathrm{m}}$ and $V_{\max}$. A special type of mixed inhibition is a non-competitive inhibition. This is the case when the inhibitor binds equally well to the free enzyme and the enzyme-substrate complex.

### 1.3.1 Inhibitory effects of substrates

Typically, increasing the substrate concentration improves the rates of enzymatic reactions. In some cases, however, the substrate binds to an enzyme or an enzyme-substrate complex in a way that prevents further catalysis. This form of inhibition can be mostly

observed at higher concentrations of the substrate when the resulting kinetics curve does not resemble a typical hyperbolic curve observed in Michaelis-Menten kinetics. There are two general ways a substrate can slow down the reaction: Non-productive binding and substrate inhibition[32].

Non-productive binding can occur when a substrate binds to an enzyme in a way that is incompatible with the catalysis, either by binding to the active site incorrectly or by binding to the secondary site in a way that renders the enzyme catalytically inactive. This model resembles competitive inhibition, with the exception that the inhibitor is the substrate. For this type of kinetics, the Michaelis-Menten equation still applies, therefore it has no easily observable effect. When unaccounted for, this can lead to underestimated $K_{\mathrm{m}}$ and $V_{\max}$ values[32].

Substrate inhibition is usually explained by an uncompetitive substrate inhibition model. This model describes a situation, where the substrate binds to a secondary site on an enzyme-substrate complex, creating an inactive enzyme-substrate-substrate complex (ESS). This resembles uncompetitive inhibition, but the inhibitor is again a substrate. This model is best described by the Haldane equation[33]:

$$v = \frac{V_{\max}[S]}{K_m + [S] + \frac{[S]^2}{K_s'}} \tag{2}$$

Where, $v$ is the initial velocity, $V_{\max}$ is the maximum velocity, $[S]$ is the substrate concentration, $K_{\mathrm{m}}$ is the Michaelis constant, and $K_{\mathrm{s}}'$ is the substrate inhibition constant. This equation states that the rate is dependent on the square of substrate concentration in the denominator, causing the rate to decline after a certain concentration value. This results in a bell-shaped kinetics curve.

# 2 Objectives of the thesis

- Preparation of Msm HelD protein using bacterial expression and purification.
- Characterization of the protein, determination of the pH optimum of ATPase and GTPase activity.
- Measurement of Michaelis curves for ATP and GTP under optimal conditions
- Discussion of the results in relation to already known facts

# 3 Methods and materials

## 3.1 Instruments

| | |
|---|---|
| **Centrifuges**: | |
| Avanti J-26S XPI | Beckman Coulter, USA |
| Centrifuge 5418 R | Eppendorf, Germany |
| Rotina 380 R | HettichLab, Germany |
| **Chromatographic columns**: | |
| HisTrapFF 5 ml | Cytiva, Sweden |
| Superdex 200 Increase 10/300 GL | Cytiva, Sweden |
| **Chromatographic system**: | |
| AKTA Pure | Cytiva, Sweden |
| **Electronic balances**: | |
| ABJ 120-4M | Kern & Sohn, Germany |
| EG 4200-2NM | Kern & Sohn, Germany |
| **Electrophoresis system**: | |
| XCell SureLock Mini-Cell Electrophoresis System | Thermo Fisher Scientific, USA |
| **Incubator**: | |
| Mini Microbiology and Hematology Incubator | Labnet, USA |
| **Laminar flow cabinet**: | |
| UVC/T-AR DNA/RNA UV-Cleaner Box | Biosan, Latvia |
| **Magnetic stirrer**: | |
| Hei-PLATE Mix 'n' Heat Core | Heidolph, Germany |
| **Microplate reader**: | |
| CLARIOstar Plus | BMG Labtech |
| **Microtitration plate**: | |
| Scientific 96-w. Brandplate 781611 | BrandTech Scientific, USA |
| **Microvolume spectrophotometer**: | |
| DS–11+ | DeNovix, USA |
| **pH meter**: | |
| Lab 855 pH Benchtop Meter | SI analytics, Germany |
| **Shaker**: | |

| | |
|---|---|
| Ecotron | Infors HT, Switzerland |
| **Sonicator**: | |
| Q700 Sonicator | QSonica, USA |

## 3.2 Materials

| | |
|---|---|
| Adenosine 5'-triphosphate disodium salt hydrate | Sigma-Aldrich, USA |
| Ammonium molybdate tetra-hydrate | Sigma-Aldrich, USA |
| Benzonase® Endonuclease | Merck Millipore, Germany |
| Bis-Tris | Sigma-Aldrich, USA |
| Carbenicillin Disodium Salt | Thermo Fischer Scientific, USA |
| Color Prestained Protein Standard(10-250 kDa) | New England BioLabs, USA |
| Dithiothreitol (DTT) | Sigma-Aldrich, USA |
| Ethylenediaminetetraacetic acid (EDTA) | Sigma-Aldrich, USA |
| Glycerol | Sigma-Aldrich, USA |
| Guanosine 5'-triphosphate sodium salt hydrate | Sigma-Aldrich, USA |
| Imidazole | Sigma-Aldrich, USA |
| InstantBlue® Coomassie Protein Stain (ISB1L) | Abcam, UK |
| L-Ascorbic acid | Sigma-Aldrich, USA |
| Lemo21 (DE3) Competent *E. coli* | New England Biolabs, USA |
| Magnesium chloride hexahydrate | Sigma-Aldrich, USA |
| NaOH | Lach-Ner, Czechia |
| Novagen™ LB Broth, Miller | Merck Millipore, Germany |
| NuPAGE™ 4-12% Bis-Tris Gel | Thermo Fisher Scientific, USA |
| NuPAGE™ MES SDS Running Buffer (20X) | Thermo Fisher Scientific, USA |
| NuPAGE™ LDS Sample Buffer (4X) | Thermo Fisher Scientific, USA |
| Overnight Express™ Instant TB Medium | Merck, Germany |
| pET302/NT-His-tag HelD (MSMEG_2174) | Prepared in our lab[21] |
| Protease Inhibitor Cocktail P8849 | Sigma-Aldrich, USA |
| Sodium Arsenite | Fisher Chemical, USA |
| Sodium chloride | Lach-Ner, Czechia |
| Sodium citrate | Sigma-Aldrich, USA |

| | |
|---|---|
| Sodium dodecyl sulfate | Sigma-Aldrich, USA |
| TEV protease | Prepared in our lab[34] |
| Trichloracetic acid | Sigma-Aldrich, USA |
| Tris (Trizma base) | Sigma-Aldrich, USA |
| tris(2-carboxyethyl)phosphine (TCEP) | Sigma-Aldrich, USA |
| Tween 20 | Sigma-Aldrich, USA |

## 3.3 Methods

### 3.3.1 Expression of Msm HelD protein

The protein was prepared by recombinant expression using already transformed cells of Lemo21 (DE3) *E. colli* containing a pET302 plasmid encoding HelD protein with N-terminal His-tag. The cells were first prepared in overnight culture in LB medium in the presence of carbenicillin (0.05 mg/ml). The next day, the cells from the overnight culture were transferred to an autoinduction medium (60 g Overnight express TB medium, 1% (w/v) glycerol in 1 l of deionized water, 50 mg carbenicillin). The mixture was incubated at 37 °C and after approximately 2 h OD 600 values were checked regularly. When OD 600 reached 0.494 the temperature was lowered to 20 °C. The cells were left in these conditions for 18 more hours. After this time the mixture was centrifuged at 5000 × g for 15 min. The supernatant was discarded and the pellet was frozen at −80 °C.

### 3.3.2 Purification of Msm HelD protein

- **Buffer A:** 15 mM imidazole, 50 mM Tris, 0.5 M NaCl, pH 7.5
- **Buffer B:** 500 mM imidazole, 50 mM Tris, 0.5 M NaCl, pH 7.5

The pellet prepared according to the purification of HelD in section 3.1 was partially defrosted and resuspended in Buffer A. After the resuspension, benzonase endonuclease (30 µl, 20 U/µl), lysozyme (100 µl, 100 mg/ml), protease inhibitors (100 µl), and Tween (50 µl) were added, total volume was approximately 25 ml. Subsequently, the cells were lysed by sonication and centrifuged (4000 × g, 10 min). The supernatant was centrifuged again (40 000 × g, 35 min), after this, the pellet was discarded.

The supernatant containing the lysate was further purified using affinity chromatography with Buffer A and Buffer B specified above. After the system and column (HisTrapFF, Cytiva) were equilibrated with Buffer A, the lysate was loaded onto the column. First, the impurities were eluted with the solution containing 5% Buffer B, and the protein was eluted with 30% Buffer B.

The eluted protein buffer was exchanged for the TEV cleavage buffer (50 mM Tris, 100 mM NaCl, 0.5 mM EDTA, 1 mM DTT, pH 7.5) using a centrifugal concentrator with a 30 kDa cut-off membrane. This resulted in 14.4 mg of protein(0.8 ml, 18.3 mg/ml). To cleave the His-tag, TEV protease was added so that the final molar ratio of TEV protease with respect to the target protein was 1:200. The mixture was left overnight to digest at 4 °C.

The buffer was then exchanged for Buffer A in the same way as described previously. Protein with the His-tag cleaved was purified by second chromatography using (HisTrap FF, Cytiva). Flow through was collected and His-tag was trapped on the column.

The buffer was exchanged for degassed Gel chromatography buffer (25 mM Tris, 100 mM NaCl, 10 mM $MgCl_2$, 1 mM TCEP), and the protein was further purified using size exclusion chromatography (Superdex 200 Increase column, Cytiva) with isocratic elution. Desired fractions were collected and stored at 4 °C.

### 3.3.3 SDS-PAGE Electrophoresis

For electrophoresis, 3 µl of sample buffer (LDS buffer with 10% (w/v) DTT) was added to samples 3–12(refer to Table 1). The protein from previous purifications was diluted to 5 µg in 10 µl (refer to the Table 1), which was then pipetted into the wells of the electrophoresis gel (NuPage 4–12% Bis-Tris, Invitrogen). The pellet of cells prepared in section 3.1 was dissolved in 40 µl of LDS and mixed with 10 µl of 10 % (w/v) SDS and 18 µl of 10% (w/v) DTT. The samples were denatured at 95 °C for 5 min.

The apparatus was assembled and filled with the running buffer. The electrophoresis was performed at 200 V and 100 mA. The gel was stained with Coomassie Brilliant Blue.

Table 1: Table of dilution of the purified protein. Protein was diluted so that the final amount in wells was 5 µg. Well 1 was the molecular weight marker, well 2 was the cell lysate, well 3 were impurities eluted at 40 mM imidazole, well 4 was eluted protein at 160 mM imidazole, well 5 was collected flow-through after His-tag cleavage, and wells from 6 to 12 were fractions collected from the SEC.

| Well | 1 | 2 | 3 | 4 | 5 | 6 | 7 | 8 | 9 | 10 | 11 | 12 |
|---|---|---|---|---|---|---|---|---|---|---|---|---|
| $V_{sample}$ [µl] | - | 13 | 10 | 0.8 | 0.625 | 0.36 | 10 | 6.66 | 1.64 | 2.4 | 3.2 | 8.45 |
| $V_{H_2O}$ [µl] | - | - | - | 9.2 | 9.375 | 9.64 | 0 | 3.34 | 8.34 | 7.6 | 6.8 | 1.55 |

### 3.3.4 Optimisation of $MgCl_2$ concentration

The same sets of reaction conditions for the HelD protein were optimized for both ATP and GTP, so in these optimisation subsections, the nucleotides will be further referred to as NTP.

To determine the optimal magnesium ion concentration for HelD activity, eight different concentrations of $MgCl_2$ were tested (0, 1, 2.5, 5, 7.5, 10, 12.5, and 15 mM). Eight individual buffers were prepared by mixing different volumes of stock 1 M $MgCl_2$ with the set volume of the stock buffer(25 mM Tris, 100 mM NaCl, pH 8).

A series of eight solutions was prepared containing the substrate (5 mM NTP) dissolved in the stock buffer mentioned above, each with a different concentration of magnesium ions. Then a second series was prepared, containing the enzyme (0.04 mg/ml) in the same series of growing magnesium concentrations.

Each measurement (in triplicates) was prepared by mixing equal volume (25 µl) of the content of individual tubes from both series. Additionally, the blank measurements were prepared in triplicates by mixing an equal volume of the substrate series with the stock buffer of the corresponding concentration of magnesium ions.

To determine the produced phosphate concentration, a duplicate of 2-fold serial dilution of inorganic phosphate in buffer (25 mM Tris, 100 mM NaCl, 7.5 mM $MgCl_2$, pH 8) was used as a calibration curve.

Prepared mixtures were incubated at 37 °C for 1 h.

### 3.3.5 Optimisation of NaCl concentration

Optimisation with respect to NaCl concentration in the activity assay was done as described previously in the section about $MgCl_2$ optimisation, except the tested concentrations of NaCl were 0, 50, 100, 200, 300, 500, 750, and 1000 mM.

### 3.3.6 pH optimisation

The pH optimum was determined by measuring the enzymatic activity of HelD in the pH range of 6–10.5, in increments of 0.5 (pH 6, 6.5, 7, 7.5, 8, 8.5, 9, 9.5, 10, and 10.5). Due to the wide range of pH, three different types of buffers had to be used. Bis-Tris buffer was used for the range of 6–7, Tris-HCl was used for the range of 7–9, and the glycine-NaOH buffer was used for the range of 9-10.5.

**Bis-Tris buffer, pH 6–7**: Stock buffer was prepared by dissolving 50 mM Bis-Tris, 1 M NaCl, and 10 mM $MgCl_2$ in 200 ml of deionized water. Individual 50 ml volumes of the stock were titrated with 5 M HCl at 37 °C to reach the desired values of pH. Each solution was adjusted to a final volume of 100 ml with deionized water.

**Tris-HCl buffer, pH 7–9**: A separate stock was prepared containing 50 mM Tris, 1 M NaCl, and 10 mM $MgCl_2$ 50 ml parts of the stock were adjusted to the desired pH values with 5 M HCl at 37 °C, then diluted to 100 ml with deionized water.

**Glycine-NaOH buffer, pH 9–10.5**: A stock of glycine-NaOH buffer was prepared(50 mM glycine, 1 M NaCl, and 10 mM $MgCl_2$). 50 ml parts of the stock were adjusted to the desired pH values with 1 M NaOH at 37 °C, and diluted to 100 ml with deionized water.

**Note:** At pH above 10, precipitation of magnesium was observed.

A series of solutions with NTP substrate and second series with HelD were prepared similar to the subsection about optimisation of $MgCl_2$ concentration, but this time in various buffers(25 mM of buffer solution depending on the pH (see above), 500 mM NaCl, 10 mM $MgCl_2$, pH 6–10.5). In microplate wells, 25 µl of solution containing substrate (5 mM NTP) was mixed with 25 µl of solution containing HelD (0.04 mg/ml) in triplicates. For background measurement, 25 µl of buffer in which each substrate was prepared was added.

To determine the produced phosphate concentration, a duplicate of 2-fold serial dilution of inorganic phosphate in buffer (25 mM Tris, 500 mM NaCl, 5 mM $MgCl_2$, pH 8) was used as a calibration curve.

Prepared mixtures were incubated at 37 °C for 1 h.

### 3.3.7 Enzyme kinetics - preparation of assay

Enzyme activity at different concentrations of the substrate was measured in optimised conditions (25 mM Tris, 500 mM NaCl, 5 mM $MgCl_2$, pH 9.0), and another measurement was done under the conditions of transcription experiments performed previously with Msm HelD[14] (25 mM Tris, 500 mM NaCl, 5 mM $MgCl_2$, pH 8). The range of substrate concentrations was achieved by a 2-fold serial dilution of NTP substrate (from 10 mM to 0.0781 mM). Each well of the microplate was filled with 25 µl of 2× concentrated substrate in triplicates. Subsequently, 25 µl of a solution containing 1 µg of HelD was added to the wells. Each set of triplicates had its triplicate of blank measurements. Buffer was added to the wells for background measurement at a 1:1 ratio, instead of the solution containing HelD.

A duplicate of a 2-fold serial dilution of inorganic phosphate was used as a calibration curve. The mixture was incubated for 30 min at 37 °C.

**Note:** To improve the tracing of the kinetics curve, a second series with 1.33-fold serial dilution of the substrate was measured simultaneously with the 2-fold dilution series. The measurements were done in duplicates because of the space constraints on the 96-well plate.

### 3.3.8 Activity assay

The assay was done by spectrophotometric determination of released phosphate. Phosphate reacts with ammonium molybdate creating phosphomolybdenium complexes which are further reduced to molybdenium blue by ascorbic acid.[35]

Enzymatic activity was measured under various conditions, each condition had its well in the microplate, in triplicate. Since both ATP and GTP may undergo spontaneous hydrolysis at different rates under different conditions, each condition had its triplicate of

background measurements.

The reagents were added to the wells after the defined reaction time in this order:

- 62 µl of reagent A: ascorbic acid (0.1 M) and trichloroacetic acid (0.5 M).
- 12.5 µl of reagent B: ammonium molybdate (0.01 M).
- 32 µl of reagent C: sodium citrate (0.1 M), sodium arsenite (0.2 M), and 5% (v/v) acetic acid.

The absorbance values were read immediately at 850 nm.

### 3.3.9 Derivation of the kinetic equation

For the analysis of the experimental kinetics data, the following reaction model was used:

$$\begin{array}{ccccc} \mathrm{E} + \mathrm{S} & \underset{k_{-1}}{\overset{k_1}{\rightleftharpoons}} & \mathrm{ES} & \xrightarrow{k_2} & \mathrm{E} + \mathrm{P} \\ + & & + & & \\ \mathrm{S_n} & & \mathrm{S_n} & & \\ \uparrow\downarrow^{K_{si}} & & \uparrow\downarrow^{K'_{si}} & & \\ \mathrm{ES_n} + \mathrm{S} & \rightleftharpoons & \mathrm{ESS_n} & & \end{array} \tag{3}$$

Just like in Michalis-Menten kinetics, the initial velocity is determined by the conversion of ES to product, which is determined by [ES]:

$$v = k_2[ES] \tag{4}$$

As ES is just a transient complex, [ES] is not easily determined. The only reliable parameter is the total enzyme concentration [$\mathrm{E_t}$]. This can be expressed as:

$$[E_t] = [E] + [ES] + [ES_i] + [ESS_i] \tag{5}$$

Under the steady-state assumption, the concentration of free enzyme [E] can be ex-

pressed in the following way:

$$k_1[E][S] = k_{-1}[ES] + k_2[ES] \tag{6}$$

$$[E] = \frac{(k_{-1} + k_2)[ES]}{k_1[S]} = K_m \frac{[ES]}{[S]} \tag{7}$$

Sums of all possible $[ES_i]$ and $[ESS_i]$ can be expressed accordingly:

$$[ES_i] = \frac{[E][S]^n}{K_{si}} \tag{8}$$

$$[ESS_i] = \frac{[ES][S]^n}{K'_{si}} \tag{9}$$

Where n is the amount of substrate molecules, which can bind to the enzyme outside of the active site. Substituting all of this to the equation of the total concentration of the enzyme gives:

$$[E_t] = K_m \frac{[ES]}{[S]} + [ES] + K_m \frac{[ES]}{[S]} \frac{[S]^n}{K_{si}} + [ES] \frac{[S]^n}{K'_{si}} \tag{10}$$

This can be simplified to:

$$[E_t] = [ES](\frac{K_m}{[S]}(1 + \frac{[S]^n}{K_{si}})) + (1 + \frac{[S]^n}{K'_{si}})) \tag{11}$$

The initial rate of the reaction can now be expressed through [ES] from Equation 4, and thus can be expressed as:

$$v = \frac{[E_t]k_2}{\frac{K_m}{[S]}(1 + \frac{[S]^n}{K_{si}})) + (1 + \frac{[S]^n}{K'_{si}})} \tag{12}$$

This can be further simplified because $[E_t]k_2$ is defined as $V_{max}$. The right side of the equation can be multiplied by a form of 1, [S]/[S]:

$$v = \frac{V_{max}[S]}{K_m(1 + \frac{[S]^n}{K_{si}}) + [S](1 + \frac{[S]^n}{K'_{si}})} \tag{13}$$

The following equation was used to fit the data using nonlinear regression in GraphPad Prism 8 (the curves were visualized in MS Excel). For the data interpretation, it can be

further simplified as follows:

$$v = \frac{V_{max}[S]}{K_m\alpha + [S]\alpha'} \tag{14}$$

Where $\alpha$ describes substrate inhibition through the binding on the free enzyme and can be expressed as:

$$(1 + \frac{[S]^n}{K_{si}}) \tag{15}$$

And $\alpha$' describes substrate inhibition through the binding on the enzyme-substrate complex. It can be expressed as:

$$(1 + \frac{[S]^n}{K'_{si}}) \tag{16}$$

# 4 Results

## 4.1 HelD expression and purification

Expression and purification of HelD yielded approximately 4.5 mg of pure protein, suitable for kinetics measurement.

The first purification step was the affinity chromatography. The obtained chromatogram (Figure 5a) combined with purity assessment(Figure 4) shows that at 40 mM imidazole, most of the impurities that did not bind to the column using the His-tag were released. Protein was eluted at 160 mM imidazole.

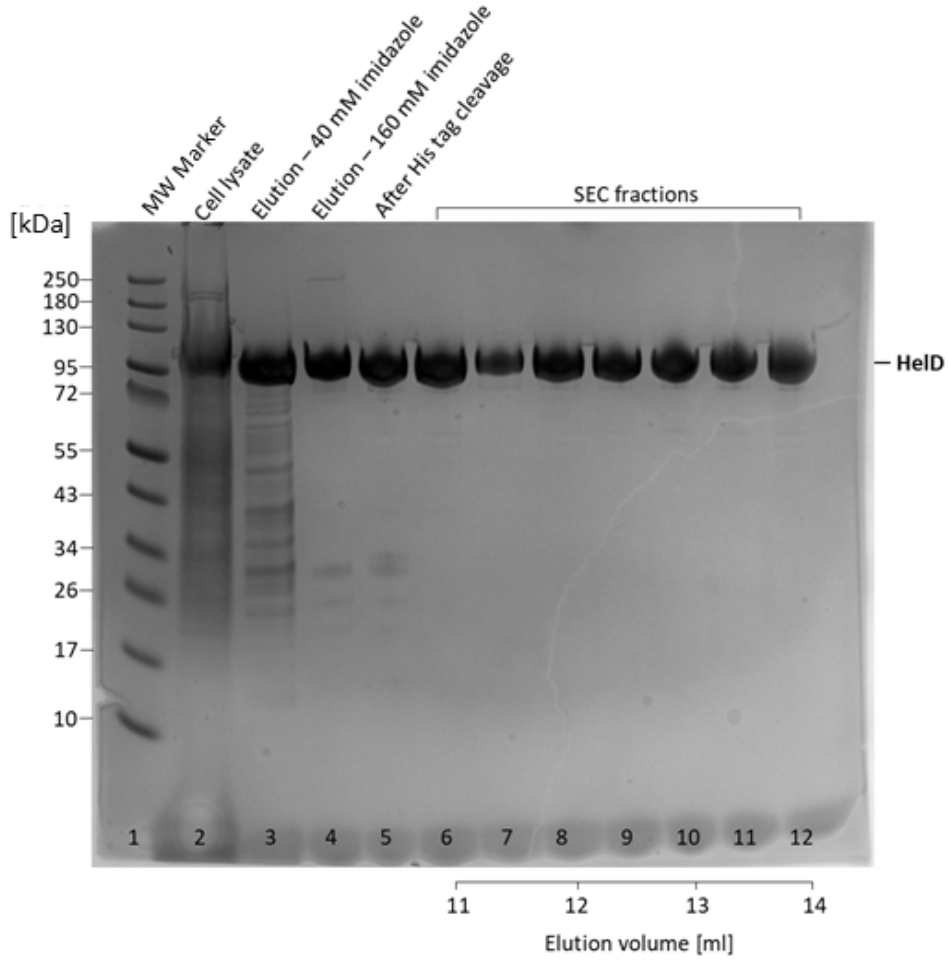


Figure 4: SDS-PAGE analysis of samples from individual purification steps. Protein concentrations in individual fractions were determined using a microvolume spectrophotometer at 280 nm. Each lane from 3–12 contained 5 µg of target protein.

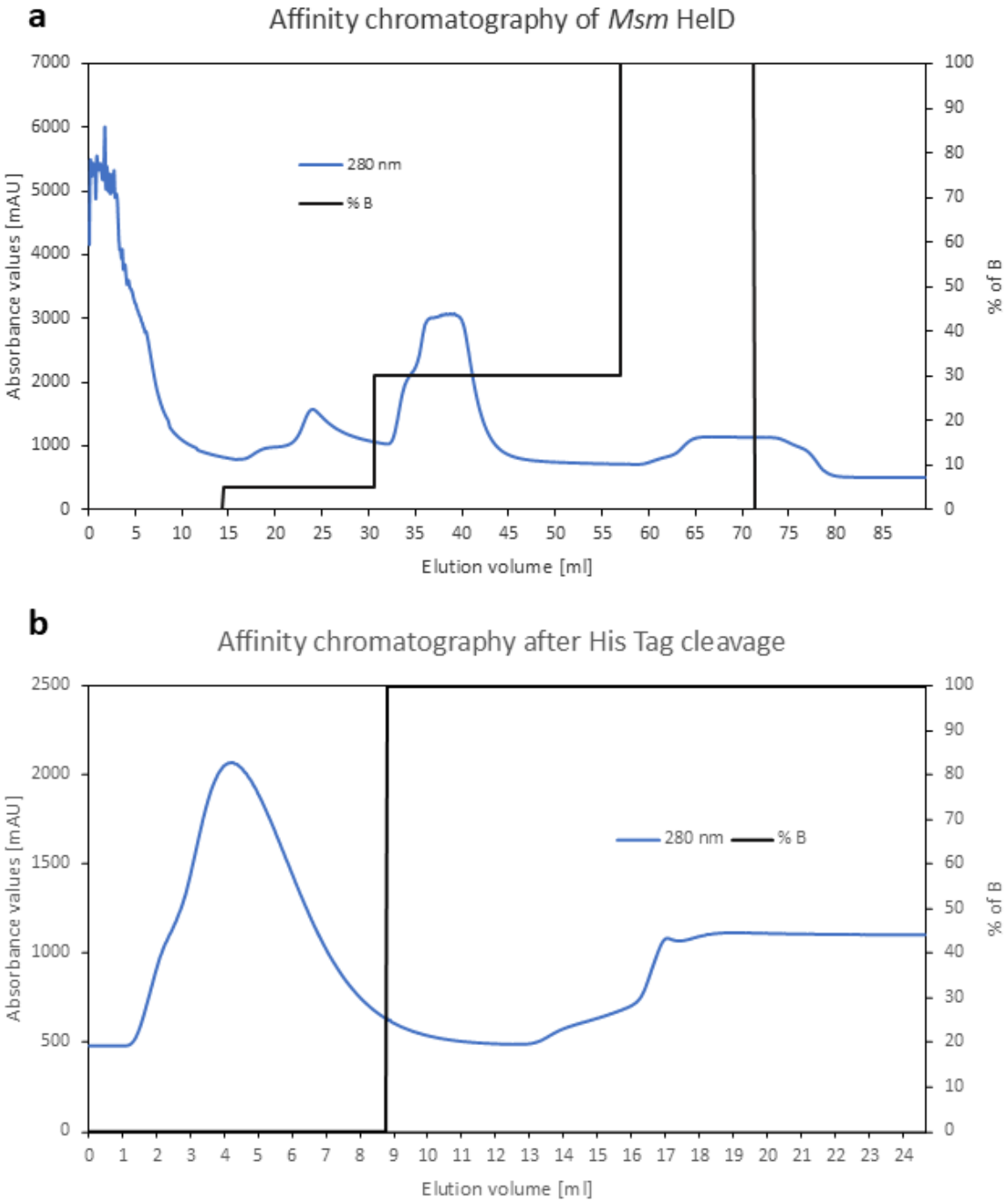


Figure 5: Affinity chromatography of Msm HelD (**a**). After lysis and centrifugation, the lysate was filtered (0.2 µm) and injected into a HisTrapFF column. First, the impurities were eluted with 5% buffer B solution and the protein was eluted with 30% buffer B solution. Buffer A: 15 mM imidazole, 50 mM Tris, 0.5 M NaCl, pH 7.5. Buffer B: 500 mM imidazole, 50 mM Tris, 0.5 M NaCl, pH 7.5. Affinity chromatography after His-tag cleavage (**b** ). After His-tag cleavage using TEV protease, the solution was loaded onto a HisTrapFF column (5 mL). Untagged HelD was immediately collected in the flow-through. Buffers A and B were the same as described above.

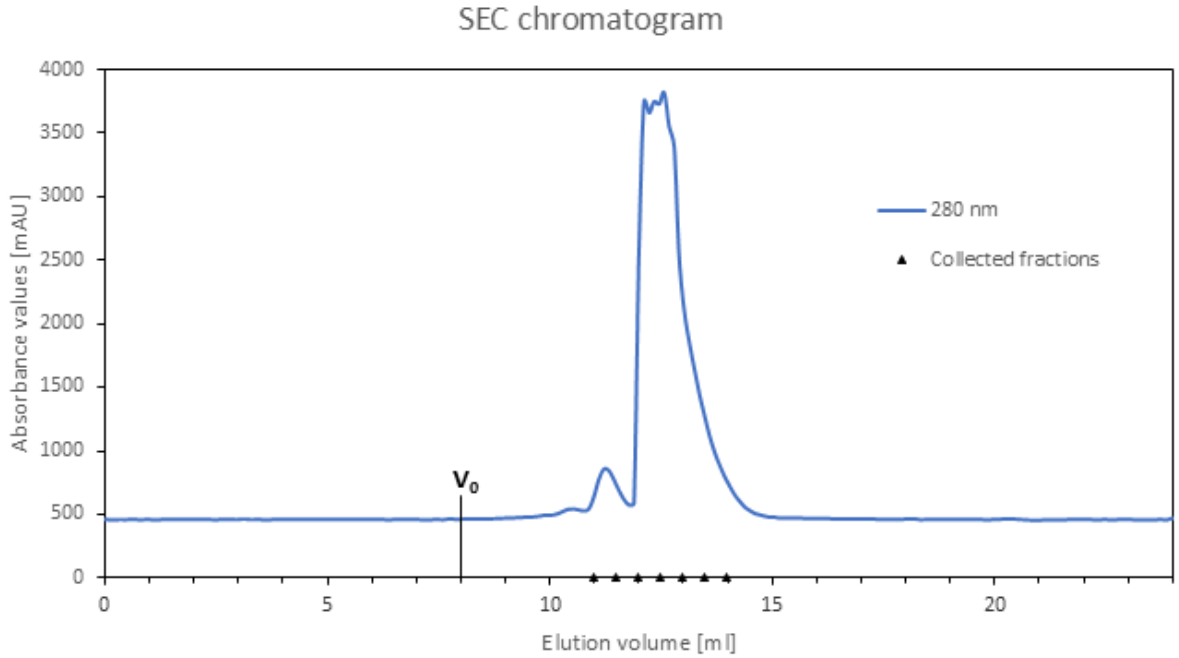


Figure 6: Size exclusion chromatography of *Msm* HelD. A Superdex 200 Increase 10/300 column (24 ml) was used, and fractions were collected every 0.5 ml. Fractions with elution volumes between 12–13 ml were used for kinetics experiments. Mobile phase: 25 mM Tris, 100 mM NaCl, 10 mM $MgCl_2$, 1 mM TCEP. The void volume of the column is 8 ml.

The chromatogram obtained after the cleavage of His-tag is shown in (Figure 5b). The chromatogram (Figure 6) of size exclusion chromatography shows one major and one minor peak. Fractions of these peaks were taken and their purity was assessed. SDS-PAGE showed (Figure 4) that their bands are approximately equal. For subsequent measurements, only the fractions at elution volumes from 12–13 ml from the major peak were taken.

## 4.2 Optimisation of $MgCl_2$ concentration

To determine the dependence of NTPase activity on $MgCl_2$ concentration, HelD activity at concentrations across a range of 0–15 mM was measured under otherwise constant conditions.

In the absence of $MgCl_2$, the enzyme showed almost no activity both for ATP (Figure 7a) and GTP(Figure 7b). The activity increases with a higher concentration of $MgCl_2$ up until 5 mM, after which it plateaues. Further optimization reactions were then carried out at 5 mM $MgCl_2$.

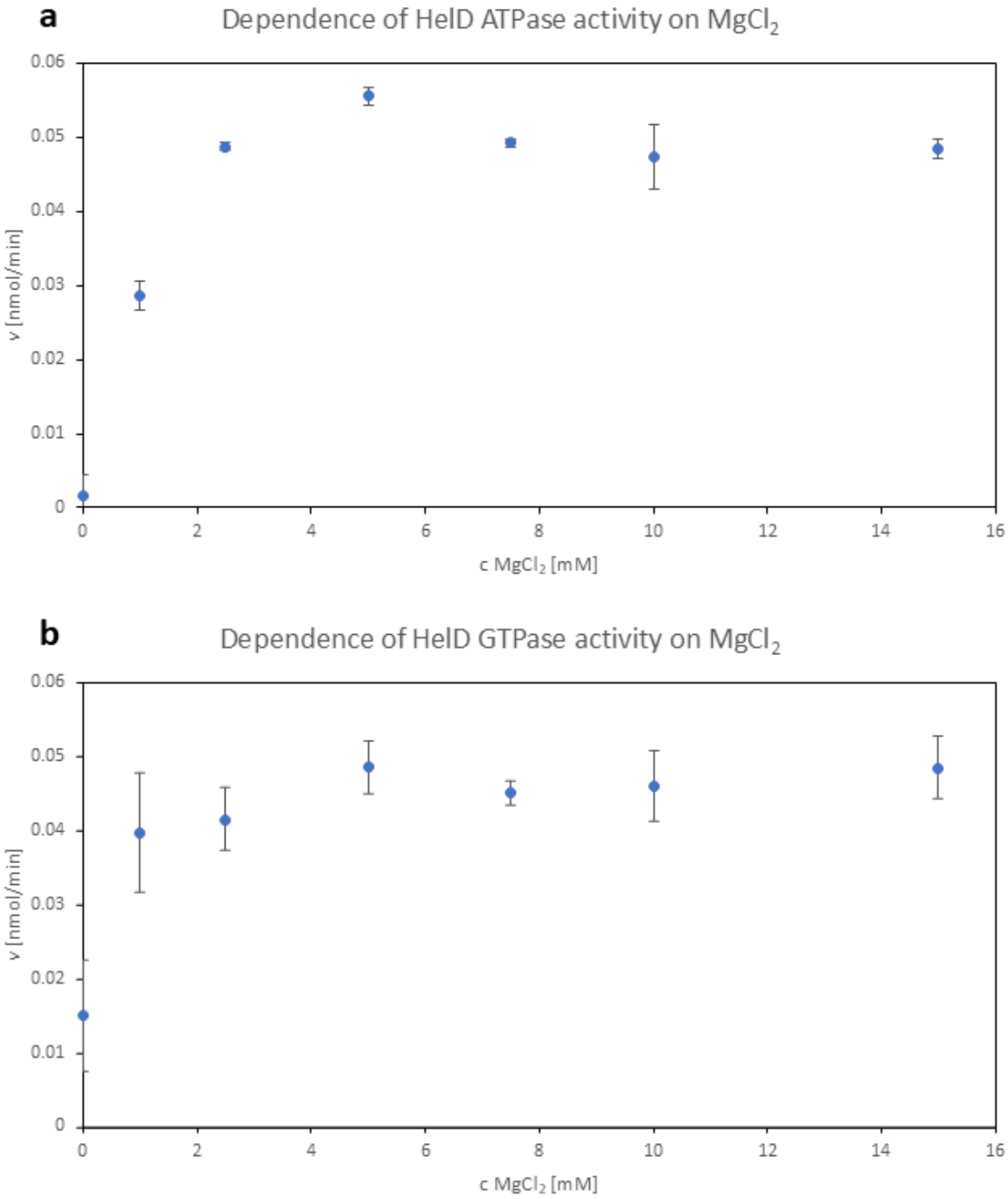


Figure 7: Dependence of HelD ATPase (**a**) and GTPase (**b**) activity on $MgCl_2$. Reaction conditions: 25 mM Tris, 100 mM NaCl, pH 8, 0–15 mM $MgCl_2$, 2.5 mM NTP, 0.02 mg/ml HelD, total volume of the reaction 50 µl, 37 °C, 1 h incubation. Error bars represent standard deviation from triplicate measurements.

## 4.3 Optimisation of NaCl concentration

To determine the impact of NaCl concentration on NTPase activities of HelD, HelD activity at concentrations across a range of 0–1 M NaCl was measured. For both ATP

(Figure 8a) and GTP (Figure 8b), activity increases up to 500 mM NaCl, before it starts to decrease.

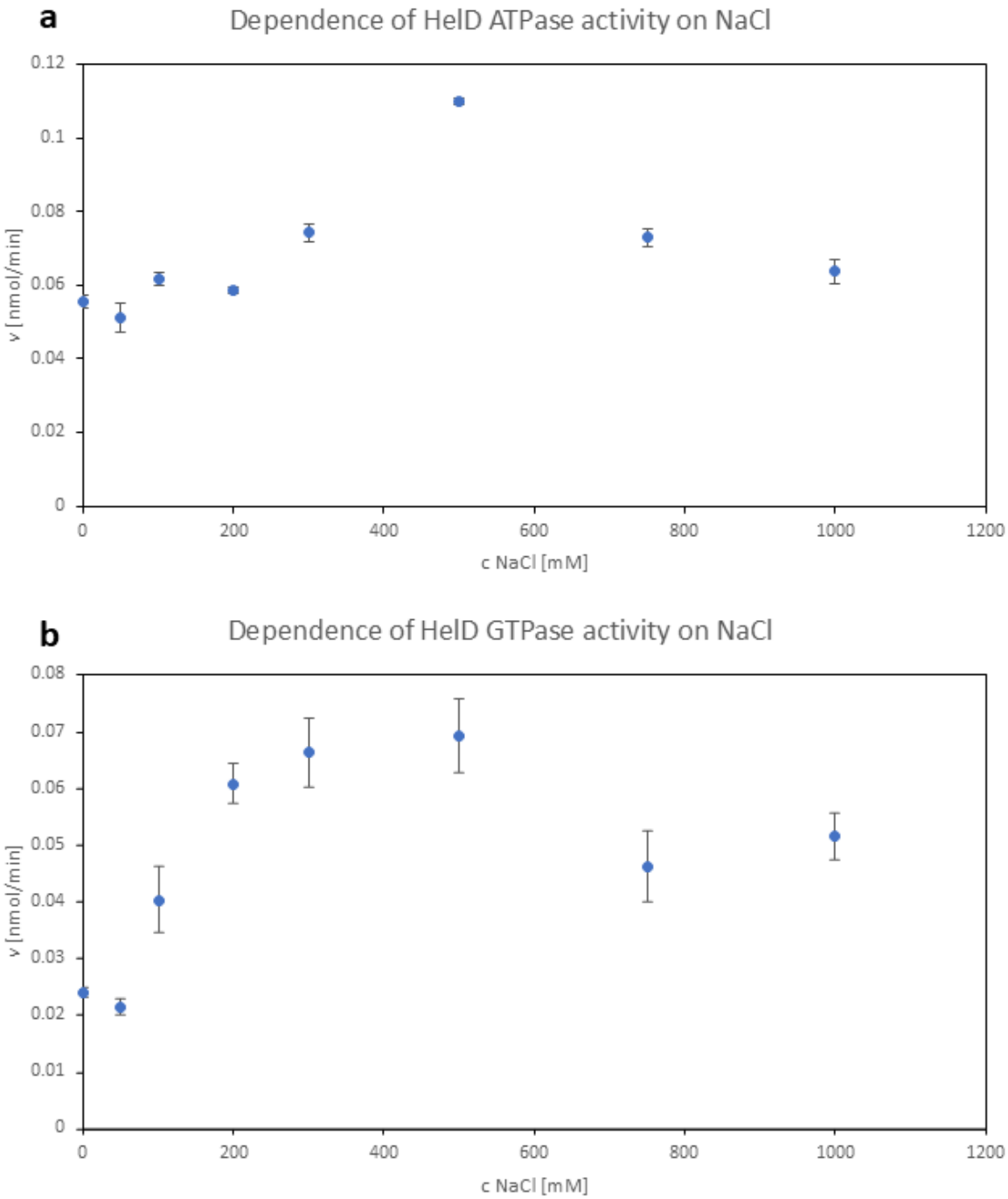


Figure 8: Dependence of HelD ATPase (**a**) and GTPase (**b**) activity on NaCl. Reaction conditions: 25 mM Tris, 0–1000 mM NaCl, pH 8, 5 mM $MgCl_2$, 2.5 mM NTP, 0.02 mg/ml HelD, total volume of the reaction 50 µl, 37 °C, 1 h incubation. Error bars represent standard deviation from triplicate measurements.

## 4.4 pH optimisation

To determine the optimal pH for NTPase activity, reactions were measured across a pH range of 7–10.5.

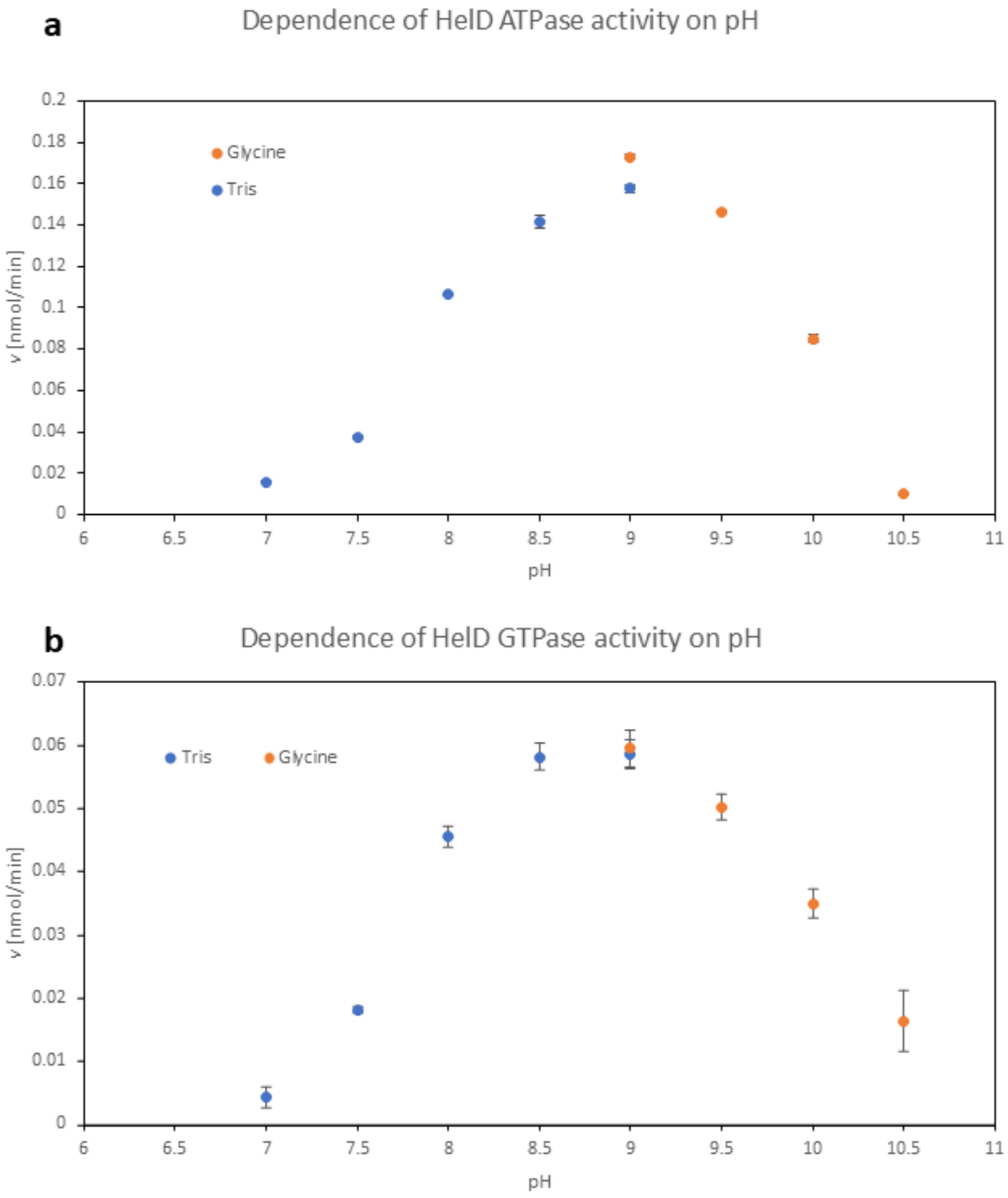


Figure 9: Dependence of HelD ATPase (**a**) and GTPase (**b**) activity on pH (7–9): 25 mM Tris, 500 mM NaCl, pH (7–9), 5 mM MgCl2, 2.5 mM NTP, 0.02 mg/ml HelD, total volume of the reaction 50 µl, 37 °C, 1 h incubation. Glycine-NaOH buffers pH (9–10.5): 25 mM Glycine, 500 mM NaCl, pH (9–10.5), 5 mM $MgCl_2$, 2.5 mM NTP, 0.02 mg/ml HelD, total volume of the reaction 50 µl, 37 °C, 1 h incubation. pH was always adjusted at 37 °C. Error bars represent standard deviation from triplicate measurements.

The pH optimum was observed at pH 9 for both ATP (Figure 9a) and GTP (Figure 9b). Although Glycine-NaOH buffer has shown higher activity, the Tris buffer was used in further measurements, because it also buffers at pH 8. at which already mentioned transcription experiments were performed.

## 4.5 Enzyme kinetics at optimal conditions

After optimization of reaction conditions, the kinetic curve was measured across a substrate concentration range of 0.07–10 mM NTP. The observed maximum of the curve was both for ATP (Figure 10a) and GTP (Figure 10b) at the substrate concentration of 2.5 mM NTP. After that point, activity decreases at higher NTP concentrations, exhibiting strong substrate inhibition. The best fit for this data is explained in Section 3.3.9.

Table 2: Fitted kinetic parameters for *Msm* HelD at pH 9 (95% confidence intervals in parentheses). It is important to note that the rate of reaction never approaches $V_{\max}$, and that $K_{\mathrm{m}}$ is not the substrate concentration, where the enzyme reaches $V_{\max}/2$, n is the number of molecules able to bind to the enzyme-substrate complex.

| Substrate | n | $V_{\max}$ [nmol/min] | $K_{\mathrm{m}}$ [mM] | $K'_{\mathrm{si}}$ |
|---|---|---|---|---|
| ATP | 3 | 0.47 (0.37–0.65) | 2.0 (1.4–3.1) | 17 (11–25) $\mathrm{mM}^3$ |
| GTP | 2 | 0.25 (0.19–0.37) | 1.3 (0.8–2.6) | 36 (18–71) $\mathrm{mM}^2$ |

Due to high $K_{\mathrm{si}}$ values for both ATP and GTP ($4 \times 10^6$ $\mathrm{mM}^3$ and $5 \times 10^8$ $\mathrm{mM}^2$ respectively), the $\alpha$ from Equation 14 can be approximated to 1. The resulting equation (Equation 14, where $\alpha$ is equal to 1), which describes uncompetitive-like substrate inhibition, was used to calculate the kinetic parameters (displayed in Table 2) from fitting this inhibition model to the experimental data.

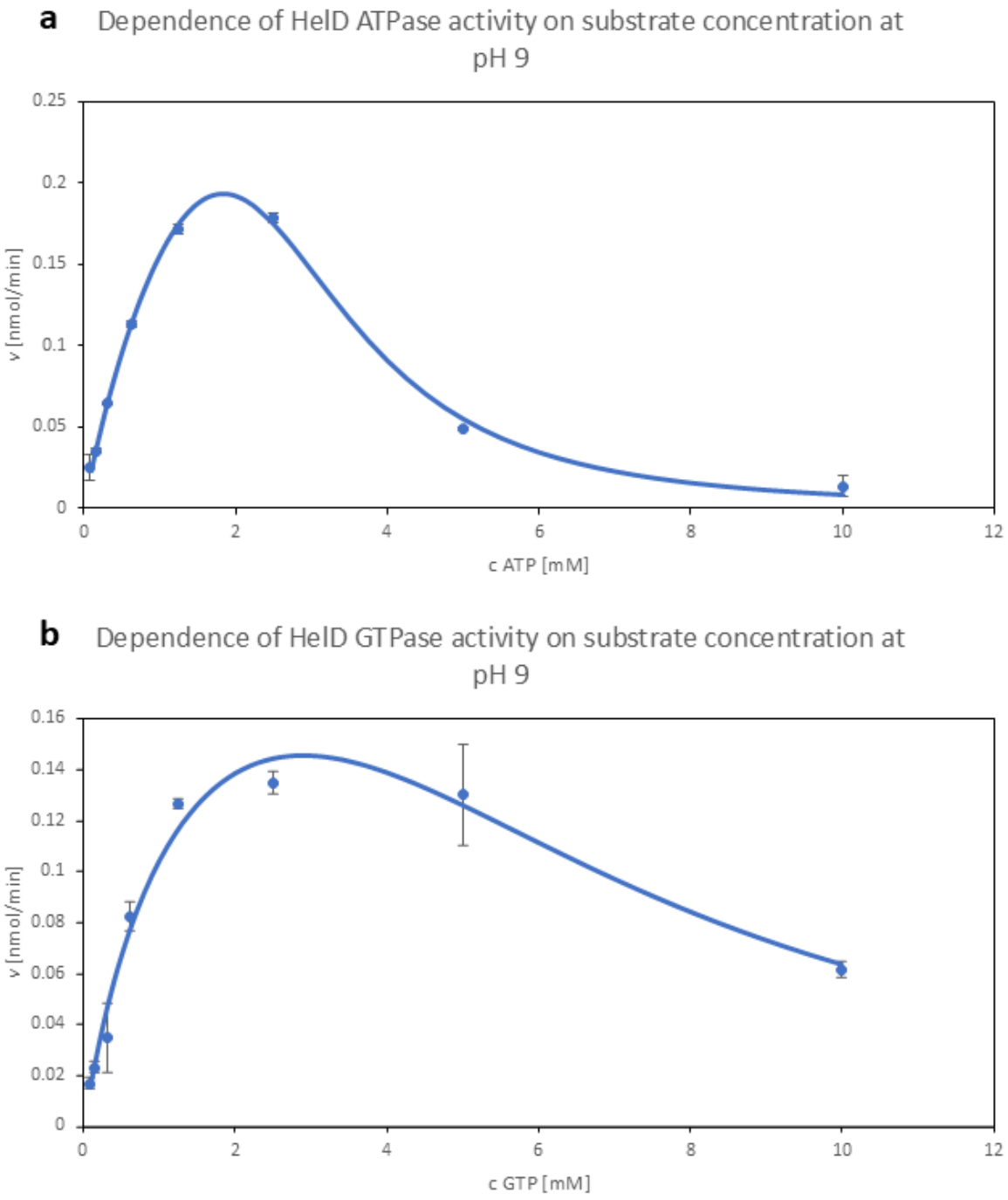


Figure 10: Reaction conditions: 25 mM Tris, 500 mM NaCl, pH 9, 5 mM $MgCl_2$, (10–0.08 mM, 2× dilution series) NTP, 0.02 mg/ml HelD, total volume of the reaction 50 µl, 37 °C, 0.5 h incubation. Error bars represent half the range of duplicate measurements, data points represent the average of two measurements.

## 4.6 Enzyme kinetics at transcription experiments conditions

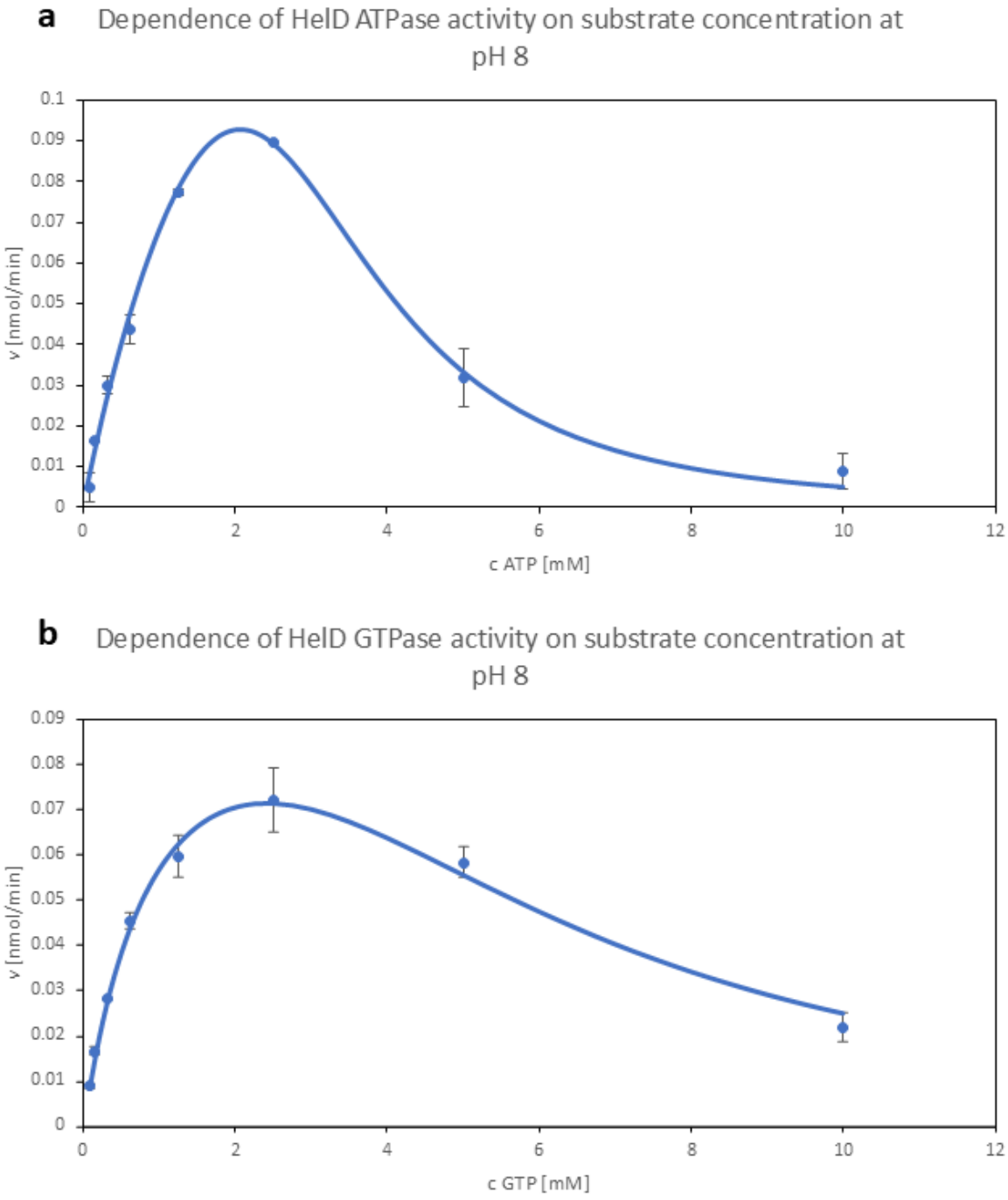


Figure 11: Dependence of HelD ATPase(**a**) and GTPase (**b**) activity on substrate concentration at pH 8. Reaction conditions: 25 mM Tris, 500 mM NaCl, pH 8, 5 mM $MgCl_2$, 10–0.08 mM NTP (2× dilution series), 0.02 mg/ml HelD, total volume of the reaction 50 µl, 37°C, 0.5 h incubation. Error bars represent half the range of duplicate measurements, data points represent the average of two measurements.

The kinetics curve was also measured at pH in which transcription experiments were undertaken. The curve shows similar substrate inhibition for both ATP (Figure 11a) and

GTP (Figure 11b) as in the pH 9 experiment.

The kinetic parameters (displayed in Table 3) were calculated in the same way as in Section 4.5.

Table 3: Fitted kinetic parameters for *Msm* HelD at pH 8 (95% confidence intervals in parentheses). The rate of reaction never approaches $V_{\max}$, and that $K_{\mathrm{m}}$ is not the substrate concentration, where the enzyme reaches $V_{\max}/2$, n is the number of molecules able to bind to the enzyme-substrate complex.

| Substrate | n | $V_{\max}$ [nmol/min]] | $K_{\mathrm{m}}$ [mM] | $K'_{\mathrm{si}}$ |
|---|---|---|---|---|
| ATP | 3 | 0.25 (0.16–0.63) | 2.0 (1.4–8.3) | 17 (7–42) $\mathrm{mM}^3$ |
| GTP | 2 | 0.12 (0.10–0.15) | 1.0 (0.7–1.6) | 36 (18–45) $\mathrm{mM}^2$ |

# 5 Discussion

The goal of this thesis was to determine the optimal reaction conditions for the HelD enzyme and to measure the kinetic curves for ATPase and GTPase activity of this enzyme.

The results show that the optimal conditions for both NTPs are 5 mM $MgCl_2$, 500 mM NaCl, and pH 9. The enzyme showed substrate inhibition, best described by an uncompetitive-like inhibition model, with the capability of the enzyme to bind three ATP molecules, or in the case of GTP, two molecules.

The enzymatic activity of HelD is performed by a conserved NTPase Rossmann fold 1A–2A heterodimer[20]. And so the closest known characterised NTPase to *Msm* HelD is *Mtb* UvrD, for which the optimal conditions are 5 mM $MgCl_2$, 50 mM NaCl, and pH 7.5[36]. Both enzymes show similar dependencies on magnesium ions, with both enzymes having optimal activity at 5 mM $MgCl_2$. However, the pH optimum and optimal concentration of NaCl differ significantly. The higher optimal NaCl concentration (500 mM) and the more basic pH (9) in the case of HelD might be explained by the differences in structural and functional properties between the two enzymes.

Unlike HelD, UvrD does not exhibit substrate inhibition, but it does have a strong dependence on nucleic acids for its activity[31]. As a helicase, UvrD is catalytically inactive in the absence of nucleic acids, which prevents unnecessary ATP hydrolysis. In contrast, HelD retains NTPase activity even when not bound to RNA polymerase, making it capable of hydrolyzing ATP independently. However, HelD significantly increases its ATPase activity upon binding to RNAP[14], possibly due to the disappearance of the substrate inhibitory effect caused by the covering of secondary binding sites. This hypothesis is consistent with the fact that 1 mM ATP releases HelD from RNAP almost as efficiently as 8 mM ATP[14], whereas free HelD exhibits maximal ATPase activity at 2.5 mM ATP and shows clear substrate inhibition at higher concentrations. Considering that the physiological concentration of ATP in *Msm* is approximately 4 mM[37], HelD can undergo structural changes, which may serve as a regulatory mechanism to prevent unnecessary ATP depletion. These structural changes may result from secondary substrate-binding sites that induce conformational changes upon binding ATP, leading to decreased enzymatic activity.

The experimental kinetic curves suggest uncompetitive substrate inhibition, a phenomenon where excess substrate binds to the enzyme-substrate complex, resulting in reduced catalytic efficiency. Upon formation of the enzyme–substrate complex, a structural shift occurs[20] that may expose secondary binding sites for the substrate. Under high substrate concentrations, these secondary sites might bind other substrate molecules, potentially inducing additional conformational changes. These changes could affect the catalytic site, leading to a decrease in enzymatic activity. Further structural studies, such as cryo-EM studies with bound substrates to these secondary sites, are required to validate this hypothesis.

# 6 Conclusion

The objectives of the thesis were reached, with the following main conclusions:

- The optimal reaction conditions for the HelD enzyme toward ATP and GTP were successfully identified as 5 mM $MgCl_2$, 500 mM NaCl, and pH 9.
- Detailed kinetic measurements were performed under the optimal conditions for pH 9 and for pH 8.
- The resulting kinetic curves revealed substrate inhibition, best described by an uncompetitive-like substrate inhibitory mechanism with multiple secondary binding sites for the substrate.
- It is known that the formation of enzyme-substrate complex leads to structural changes of HelD, which might allow additional substrate molecules to bind to these secondary binding sites.
- Kinetic parameters were calculated by fitting this model to the data (Table 2 and 3), with about double the values of $V_{\max}$ and $K_{\mathrm{m}}$ with ATP as substrate compared to GTP at both pH points. While the $K_{\mathrm{m}}$ values stay the same when comparing catalysis at pH 9 and 8, the $V_{\max}$ values decrease to about 50% of the pH 9 values.
- HelD slightly prefers ATP to GTP as a substrate at pH 9 and pH 8, when judged by overall kinetic parameters.
- The observed substrate inhibition could be a regulatory mechanism to prevent unnecessary NTP hydrolysis by HelD when not bound to RNA polymerase.

# References


[1] Sutherland, C.; Murakami, K. S. An Introduction to the Structure and Function of the Catalytic Core Enzyme of Escherichia coli RNA Polymerase. *EcoSal Plus*; **8**:1, 10.1128/ecosalplus.ESP-00042018. (2018). https://doi.org/10.1128/ecosalplus.esp-0004-2018.

[2] Österberg, S.; Peso-Santos, T. D.; Shingler, V. Regulation of Alternative Sigma Factor Use. *Annual Review of Microbiology*; **65**:1, 37-55. (2011). https://doi.org/10.1146/annurev.micro.112408.134219.

[3] Nelson, D. L.; Cox, M. M.; Lehninger, A. L. Lehninger principles of biochemistry. 6th ed. New York, NY: Freeman. ISBN: 978-1-4641-0962-1.

[4] Govindarajan, S.; Amster-Choder, O. Transcription Regulation in Bacteria. In: Schmidt, T. M., editor. Encyclopedia of Microbiology (Fourth Edition). Oxford: Academic Press. (2019). p. 441-57. https://doi.org/10.1016/B978-0-12-801238-3.02462-4.

[5] Zhang, G.; Campbell, E. A.; Minakhin, L.; Richter, C.; Severinov, K.; Darst, S. A. Crystal Structure of Thermus aquaticus Core RNA Polymerase at 3.3 Å Resolution. *Cell*; **98**:6, 811-24. (1999). https://doi.org/10.1016/S0092-8674(00)81515-9.

[6] Burgess, R. R.; Travers, A. A.; Dunn, J. J.; Bautz, E. K. F. Factor Stimulating Transcription by RNA Polymerase. *Nature*; **221**:5175, 43-6. (1969). https://doi.org/10.1038/221043a0.

[7] Paget, M. S. Bacterial Sigma Factors and Anti-Sigma Factors: Structure, Function and Distribution. *Biomolecules*; **5**:3, 1245-65. (2015). https://doi.org/10.3390/biom5031245.

[8] Browning, D. F.; Busby, S. J. W. Local and global regulation of transcription initiation in bacteria. *Nature Reviews Microbiology*; **14**:10, 638-50. (2016). https://doi.org/10.1038/nrmicro.2016.103.

[9] Krásný, L.; Gourse, R. L. An alternative strategy for bacterial ribosome synthesis: Bacillus subtilis rRNA transcription regulation. *The EMBO Journal*; **23**:22, 4473-83. (2004). https://doi.org/10.1038/sj.emboj.7600423.

[10] Hnilicová, J.; Jirát Matějčková, J.; Šiková, M.; Pospíšil, J.; Halada, P.; Pánek, J.; Krásný, L. Ms1, a novel sRNA interacting with the RNA polymerase core in mycobacteria. *Nucleic Acids Research*; **42**:18, 11763-76. (2014). https://doi.org/10.1093/nar/gku793.

[11] Brantl, S.; Licht, A. Characterisation of Bacillus subtilis Transcriptional Regulators Involved in Metabolic Processes. *Current Protein & Peptide Science*; **11**:4, 274-91. https://doi.org/10.2174/138920310791233396.

[12] Weiss, A.; Shaw, L. N. Small things considered: the small accessory subunits of RNA polymerase in Gram-positive bacteria. *FEMS Microbiology Reviews*; **39**:4, 541-54. (2015). https://doi.org/10.1093/femsre/fuv005.

[13] Hauryliuk, V.; Atkinson, G. C.; Murakami, K. S.; Tenson, T.; Gerdes, K. Recent

functional insights into the role of (p)ppGpp in bacterial physiology. *Nature Reviews Microbiology*; **13**:5, 298-309. (2015). https://doi.org/10.1038/nrmicro3448.

[14] Kovaľ, T.; Borah, N.; Sudzinová, P.; Brezovská, B.; Šanderová, H.; Vaňková Hausnerová, V.; Křenková, A.; Hubálek, M.; Trundová, M.; Adámková, K.; Dušková, J.; Schwarz, M.; Wiedermannová, J.; Dohnálek, J.; Krásný, L.; Kouba, T. Mycobacterial HelD connects RNA polymerase recycling with transcription initiation. *Nature Communications*; **15**:1, 8740. (2024). https://doi.org/10.1038/s41467-024-52891-5.

[15] Delumeau, O.; Lecointe, F.; Muntel, J.; Guillot, A.; Guédon, E.; Monnet, V.; Hecker, M.; Becher, D.; Polard, P.; Noirot, P. The dynamic protein partnership of RNA polymerase inBacillus subtilis. *PROTEOMICS*; **11**:15, 2992-3001. (2011). https://doi.org/10.1002/pmic.201000790.

[16] Wiedermannová, J.; Sudzinová, P.; Kovaľ, T.; Rabatinová, A.; Šanderová, H.; Ramaniuk, O.; Rittich, ; Dohnálek, J.; Fu, Z.; Halada, P.; Lewis, P.; Krásný, L. Characterization of HelD, an interacting partner of RNA polymerase from Bacillus subtilis. *Nucleic Acids Research*; **42**:8, 5151-63. (2014). https://doi.org/10.1093/nar/gku113.

[17] Yang, W. Lessons Learned from UvrD Helicase: Mechanism for Directional Movement*. *Annual Review of Biophysics*; **39**, 367-85. (2010). https://doi.org/10.1146/annurev.biophys.093008.131415.

[18] Carrasco, B.; Fernández, S.; Petit, M.-A.; Alonso, J. C. Genetic Recombination in Bacillus subtilis 168: Effect of ΔhelD on DNA Repair and Homologous Recombination. *Journal of Bacteriology*; **183**:19, 5772-7. (2001). https://doi.org/10.1128/jb.183.19.5772-5777.2001.

[19] Kaur, G.; Kapoor, S.; Thakur, K. G. Bacillus subtilis HelD, an RNA Polymerase Interacting Helicase, Forms Amyloid-Like Fibrils. *Frontiers in Microbiology*; **9**. (2018). https://doi.org/10.3389/fmicb.2018.01934.

[20] Kovaľ, T.; Sudzinová, P.; Perháčová, T.; Trundová, M.; Skálová, T.; Fejfarová, K.; Šanderová, H.; Krásný, L.; Dušková, J.; Dohnálek, J. Domain structure of HelD, an interaction partner of Bacillus subtilis RNA polymerase. *FEBS Letters*; **593**:9, 996-1005. (2019). https://doi.org/10.1002/1873-3468.13385.

[21] Kouba, T.; Koval', T.; Sudzinová, P.; Pospíšil, J.; Brezovská, B.; Hnilicová, J.; Šanderová, H.; Janoušková, M.; Šiková, M.; Halada, P.; Sýkora, M.; Barvík, I.; Nováček, J.; Trundová, M.; Dušková, J.; Skálová, T.; Chon, U.; Murakami, K. S.; Dohnálek, J.; Krásný, L. Mycobacterial HelD is a nucleic acids-clearing factor for RNA polymerase. *Nature Communications*; **11**:1, 6419. (2020). https://doi.org/10.1038/s41467-020-20158-4.

[22] Giddey, A. D.; de Kock, E.; Nakedi, K. C.; Garnett, S.; Nel, A. J. M.; Soares, N. C.; Blackburn, J. M. A temporal proteome dynamics study reveals the molecular basis of induced phenotypic resistance in Mycobacterium smegmatis at sub-lethal rifampicin concentrations. *Scientific Reports*; **7**:1, 43858. (2017). https://doi.org/10.1038/srep43858.

[23] Hurst-Hess, K. R.; Saxena, A.; Rudra, P.; Yang, Y.; Ghosh, P. My-

cobacterium abscessus HelR interacts with RNA polymerase to confer intrinsic rifamycin resistance. *Molecular Cell*; **82**:17, 3166-77.e5. (2022). https://doi.org/10.1016/j.molcel.2022.06.034.

[24] Surette, M. D.; Waglechner, N.; Koteva, K.; Wright, G. D. HelR is a helicase-like protein that protects RNA polymerase from rifamycin antibiotics. *Molecular Cell*; **82**:17, 3151-65.e9. (2022). https://doi.org/10.1016/j.molcel.2022.06.019.

[25] Larsen, J. S.; Miller, M.; Oakley, A. J.; Dixon, N. E.; Lewis, P. J. Multiple classes and isoforms of the RNA polymerase recycling motor protein HelD. *MicrobiologyOpen*; **10**:6, e1251. (2021). https://doi.org/10.1002/mbo3.1251.

[26] Lin, W.; Das, K.; Degen, D.; Mazumder, A.; Duchi, D.; Wang, D.; Ebright, Y. W.; Ebright, R. Y.; Sineva, E.; Gigliotti, M.; Srivastava, A.; Mandal, S.; Jiang, Y.; Liu, Y.; Yin, R.; Zhang, Z.; Eng, E. T.; Thomas, D.; Donadio, S.; Zhang, H.; Zhang, C.; Kapanidis, A. N.; Ebright, R. H. Structural Basis of Transcription Inhibition by Fidaxomicin (Lipiarmycin A3). *Molecular Cell*; **70**:1, 60-71.e15. (2018). https://doi.org/10.1016/j.molcel.2018.02.026.

[27] Boyaci, H.; Chen, J.; Lilic, M.; Palka, M.; Mooney, R. A.; Landick, R.; Darst, S. A.; Campbell, E. A. Fidaxomicin jams Mycobacterium tuberculosis RNA polymerase motions needed for initiation via RbpA contacts. *eLife*; **7**, e34823. (2018). https://doi.org/10.7554/eLife.34823.

[28] Lin, W.; Mandal, S.; Degen, D.; Liu, Y.; Ebright, Y. W.; Li, S.; Feng, Y.; Zhang, Y.; Mandal, S.; Jiang, Y.; Liu, S.; Gigliotti, M.; Talaue, M.; Connell, N.; Das, K.; Arnold, E.; Ebright, R. H. Structural Basis of Mycobacterium tuberculosis Transcription and Transcription Inhibition. *Molecular Cell*; **66**:2, 169-79.e8. (2017). https://doi.org/10.1016/j.molcel.2017.03.001.

[29] Campbell, E. A.; Korzheva, N.; Mustaev, A.; Murakami, K.; Nair, S.; Goldfarb, A.; Darst, S. A. Structural Mechanism for Rifampicin Inhibition of Bacterial RNA Polymerase. *Cell*; **104**:6, 901-12. (2001). https://doi.org/10.1016/S0092-8674(01)00286-0.

[30] Sudzinová, P.; Šanderová, H.; Koval', T.; Skálová, T.; Borah, N.; Hnilicová, J.; Kouba, T.; Dohnálek, J.; Krásný, L. What the Hel: recent advances in understanding rifampicin resistance in bacteria. *FEMS Microbiology Reviews*; **47**:6, fuac051. (2023). https://doi.org/10.1093/femsre/fuac051.

[31] Lee, J. Y.; Yang, W. UvrD Helicase Unwinds DNA One Base Pair at a Time by a Two-Part Power Stroke. *Cell*; **127**:7, 1349-60. (2006). https://doi.org/10.1016/j.cell.2006.10.049.

[32] Cornish-Bowden, A. Fundamentals of enzyme kinetics. Third ed ed. London: Portland press. ISBN: 978-1-85578-158-0.

[33] Sonnad, J. R.; Goudar, C. T. Solution of the Haldane equation for substrate inhibition enzyme kinetics using the decomposition method. *Mathematical and Computer Modelling*; **40**:5, 573-82. (2004). https://doi.org/10.1016/j.mcm.2003.10.051.

[34] Koehn, J.; Hunt, I. High-Throughput Protein Production (HTPP): A Review of Enabling Technologies to Expedite Protein Production. In: Doyle, S. A., editor. High

Throughput Protein Expression and Purification: Methods and Protocols. Totowa, NJ: Humana Press. (2009). p. 1-18. https://doi.org/10.1007/978-1-59745-196-3.

[35] He, Z.; ; Honeycutt, C. W. A Modified Molybdenum Blue Method for Orthophosphate Determination Suitable for Investigating Enzymatic Hydrolysis of Organic Phosphates. *Communications in Soil Science and Plant Analysis*; **36**:9-10, 1373-83. (2005). https://doi.org/10.1081/CSS-200056954.

[36] Curti, E.; Smerdon, S. J.; Davis, E. O. Characterization of the Helicase Activity and Substrate Specificity of Mycobacterium tuberculosis UvrD. *Journal of Bacteriology*; **189**:5, 1542-55. (2007). https://doi.org/10.1128/JB.01421-06.

[37] Knejzlík, Z.; Doležal, M.; Herkommerová, K.; Clarova, K.; Klíma, M.; Dedola, M.; Zborníková, E.; Rejman, D.; Pichová, I. The mycobacterial guaB1 gene encodes a guanosine 5-monophosphate reductase with a cystathionine-β-synthase domain. *The FEBS Journal*; **289**:18, 5571-98. (2022). https://doi.org/10.1111/febs.16448.